DOI: 10.1002/chem.200500138

Cationic P–S–X cages (X = Br, I)

Marcin Gonsior,[a] Ingo Krossing,*[b] and Eberhard Matern[a]

Abstract: The first condensed-phase preparation of ternary P–Ch–X cations (Ch = O–Te, X = F–I) is reported: $[P_5S_3X_2]^+$, $[P_5S_2X_2]^+$, and $[P_4S_4X]^+$ (X = Br, I). $[P_5S_3X_2]^+$ is formed from the reaction of the Ag^+/PX_3 reagent with P_4S_3. The $[P_5S_3X_2]^+$ ions have a structure that is related to P_4S_5 by replacing P=S by P^+–X and S in the four-membered ring by P(X). We provide evidence that the active ingredient of the Ag^+/PX_3 reagent is the $(H_2CCl_2)Ag–X–PX_2^+$ cation. The latter likely reacts with the HOMO of P_4S_3 in a concerted HOMO–LUMO addition to give the $P_5S_3X_2^+$ ion as the first species visible in situ in the low-temperature ^{31}P NMR spectrum. The $[P_5S_3X_2]^+$ ions are metastable at −78 °C and disproportionate at slightly higher temperatures to give $[P_5S_2X_2]^+$ and $[P_4S_4X]^+$, probably with the extrusion of $1/n(PX)_n$ (X = Br, I). All six new cage compounds have been characterized by multinuclear NMR spectroscopy and, in part, by IR or Raman spectroscopy. The $[P_5S_2X_2]^+$ salts have a nortricyclane skeleton and were also characterized by X-ray crystallography. The structure of the $[P_4S_4X]^+$ ion is related to that of P_4S_5 in that the *exo*-cage P=S bond is replaced by an isoelectronic P^+–X moiety.

Keywords: cage compounds · cations · phosphorus · silver · sulfur

Introduction

Hitherto about 19 different binary tetraphosphorus sulfide molecules P_4S_n (n = 3–10) are known. Of these, P_4S_3 and P_4S_{10} are used on a multi-ton scale.[1] Polymeric $(P_4S_n)_\infty$ varieties are unknown. Other binary compositions such as P_xS_n ($x \neq 4$) are unknown in the condensed phase, except for a compound that is thought to be polymeric PS.[2] Ternary trivalent polyphosphorus sulfides such as P_5S_2Y (Y = H, NMePh, SPh, PPh, Cl, Br, I)[3,4] and P_6SY_2 (Y = I)[4] are less common and, apart from α- and β-$P_4S_3I_2$, structurally uncharacterized.[5–8] The only other ternary phosphorus sulfides known are of the type S=PX_3, X = F-I (also mixed halides). Ionic polyphosphorus–sulfur cages are less well explored than the respective neutral compounds. Some rare examples have been observed inside a mass spectrometer, but there are no structurally characterized anionic binary P–S or ternary P–S–Y cages. This is astonishing considering the large number of investigations on the related P_n^{x-} polyphosphides.[9–13] Binary P–Ch and ternary P–Ch–X cations (Ch = O–Te, X = F–I) remain unknown in the condensed phase, the As–S cation $As_3S_4^+$ being the only related example that is known.[14] All earlier attempts to synthesize P_x^+ and $P_xS_y^+$ ions failed.[15] Hitherto applied counterions like MF_6^- (M = As, Sb) decompose in the presence of P-containing cations with liberation of PF_3. This should be contrasted with the multitude of lighter homologous binary N–S and ternary N–S–X cations known that are stable in the presence of MF_6^- ions. Therefore, it appears that a new preparative route and another weakly coordinating anion (WCA) are prerequisites for the successful synthesis of binary and ternary P–S(–X) cations.

Herein we report a method for the preparation of ternary P–S–X cations (X = Br, I) with the perfluorinated alkoxyaluminate $[Al(OR)_4]^-$ as a counterion (R = $C(CF_3)_3$).[15–26] Reaction of the Ag^+/PX_3 reagent[16,22,25,27] with P_4S_3 leads to the cations $P_5S_3X_2^+$, $P_4S_4X^+$, and $P_5S_2X_2^+$ (X = Br, I).

Results

Synthesis: Depending on the temperature, three halogen-containing salts **1–3** (Figure 1) are obtained from P_4S_3, PX_3, and $Ag[Al(OR)]_4$, namely $P_5S_3X_2^+[Al(OR)]_4^-$ at −78 °C

[a] Dr. M. Gonsior, Dr. E. Matern
Universität Karlsruhe (TH), Institut für Anorganische Chemie
Engesserstrasse Geb. 30.45, 76128 Karlsruhe (Germany)

[b] Prof. I. Krossing
Ecole Polytechnique Fédérale de Lausanne (EPFL),
Laboratory of Inorganic and Coordination Chemistry (LCIC),
ISIC-BCH, 1015 Lausanne (Switzerland)
E-mail: ingo.krossing@epfl.ch

Supporting information for this article is available on the WWW under http://www.chemeurj.org/ or from the author.

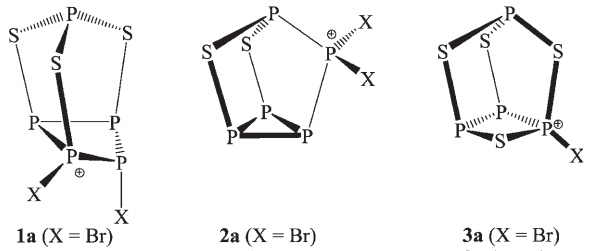

1a (X = Br) **2a** (X = Br) **3a** (X = Br)
1b (X = I) **2b** (X = I) **3b** (X = I)

Figure 1. Structures of the cationic P–S–X cages in **1a**,**b**, **2a**,**b**, and **3a**,**b**.

[X = Br **1a**, I **1b**, Eq. (1)], $P_5S_2X_2^+[Al(OR)]_4^-$ [X = Br **2a**, I **2b**, Eq. (2)] also at −78 °C, and $P_4S_4X^+[Al(OR)]_4^-$ [X = Br **3a**, I **3b**, Eq. (3)] at −30 °C.

$$P_4S_3 + PX_3 + Ag[Al(OR)_4] \xrightarrow{-78^\circ C,\ CH_2Cl_2} Ag(P_4S_3)(PX_3)^+[Al(OR)_4]^- \quad (1)$$

$$Ag(P_4S_3)(PX_3)^+[Al(OR)_4]^- \xrightarrow{-78^\circ C,\ CH_2Cl_2} P_5S_3X_2^+[Al(OR)_4]^- + AgX \quad (2)$$

$$P_5S_3X_2^+[Al(OR)_4]^- + AgX \xrightarrow{-30^\circ C\ \text{to RT},\ CH_2Cl_2} 0.5\ P_5S_2X_2^+[Al(OR)_4]^- + 0.5\ P_4S_4X^+[Al(OR)_4]^- + {}^1/_{2n}(PX)_n + AgX \quad (3)$$

The reaction proceeds initially by complex formation between Ag^+, P_4S_3, and PBr_3 [Eq. (1)]. The dynamic and exchanging $[Ag(P_4S_3)(PBr_3)]^+$ complex has a sufficiently long lifetime at −78 °C to be observed in the ^{31}P NMR spectrum (broad lines for PBr_3 and P_4S_3; see Supporting Information).

We assume a similar situation for Ag^+, P_4S_3, and PI_3. However, no signal due to coordinated PI_3 was observed, which may be due to the low solubility of PI_3 at −78 °C and the immediate elimination of AgI from the $[Ag(P_4S_3)(PI_3)]^+$ intermediate [Eq. (3)]. The presence of $P_5S_3X_2^+$ ions was confirmed by the ^{31}P NMR spectra of NMR-scale reactions that were always kept at −78 °C. The reactions leading to **1a** and **1b** proceed selectively at −78 °C to give only one $P_5S_3X_2^+$ isomer (no mixture, see X = I in Figure 2).

Assignment of the correct structure to **1a**,**b** (Figure 1) was difficult (see Discussion) as only a P–X disruptive addition of a PX_2^+ moiety to P_4S_3 led to a structure that is in good agreement with available related experimental as well as calculated data. (For related NMR calculations see references [3,28]) At this point we have to thank one of the referees, who correctly suggested that we reconsider our initially proposed structure for **1a**,**b**.

Upon trying to grow crystals of **1a**,**b** at −30 °C we only isolated crystals of **2a**,**b**, which have one S atom less in the skeleton than **1a**,**b**, such that **2a**,**b** have a structure that is isoelectronic to that of P_4S_3 in which one S atom has been replaced by a PX_2^+ unit (Figure 1). Compounds **1a**,**b** dismutate in solution at temperatures above −78 °C. The formation of **1b** is complete after three weeks at −78 °C, and almost no signals other than those of **1b** are observed in the NMR spectrum (Figure 2). However, after this three-week period, or when the temperature is increased for a few minutes to room temperature, the signals of the dismutation products **2b** and **3b** appear with increasing intensity. The dismutation of **1a** proceeds analogously to give **2a** and **3a**. The rates of the dismutation reactions of **1a** and **1b**, however, are different, and **1b** converts faster than its Br analogue **1a**: only **2b** and **3b** are observed in the ^{31}P NMR spectrum after about 20–30 minutes at room temperature or after 1–2

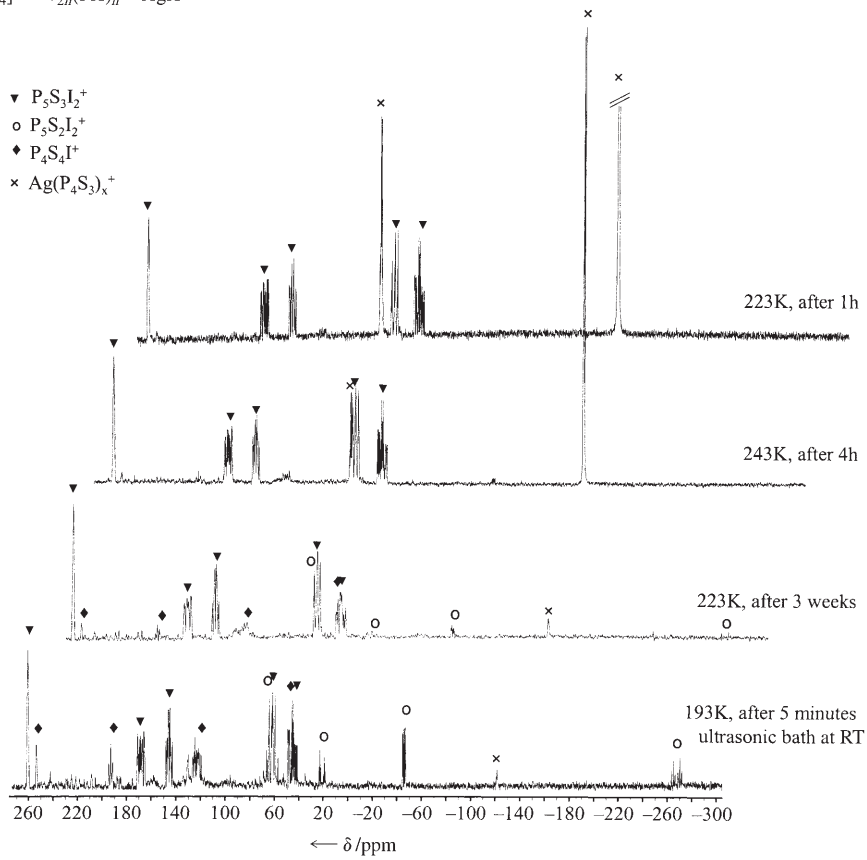

Figure 2. Progress of the reaction between PI_3, P_4S_3, and $Ag[Al(OR)_4]$ in the ^{31}P NMR spectrum. Uncomplexed PI_3 and P_4S_3 are insoluble in CD_2Cl_2 at low temperature and are not observed. The signals at $\delta = +75.1$ (q, $^2J_{P,P} = 62.6$ Hz) and −125.2 ppm ($^2J_{P,P} = 62.3$ Hz) belong to $Ag(P_4S_3)_x^+$.[23]

weeks at −30 °C, whereas **1a** is still present in the ^{31}P NMR spectrum after several weeks at −30 °C. If the sample is kept at 0 °C, the conversion of **1a** to **2a** and **3a** proceeds within 1–2 days and is accompanied by some anion decomposition, which is indicative that **1a** is more reactive than **1b** (formation of the $[(RO)_3Al–F–Al(OR)_3]^-$ ion is detected by NMR spectroscopy, see earlier work).[15,22,29] No decomposition of the anion was detected for **1b** or its disproportionation products **2b** and **3b**, even when the solution was handled at ambient temperature. Since the salts **1a** and **1b** are only metastable, the isolation of pure solid products was not possible, not even when the reactions were performed in a CS_2/CH_2Cl_2 solvent mixture. Solid **2a**, **2b**, and **3a** (**2a** as a mixture with **3a**) were obtained in good yields and were characterized by IR and, in part, also by Raman spectroscopy, as well as by an X-ray single-crystal structure analysis for **2a,b**.

Table 1. Experimental and MPW1PW91/6-311G(2df) calculated ^{31}P NMR shifts and coupling constants of the cations of **1a**, **1b**, **3a**, and **3b**.

	1a exptl[a]	**1a** calcd[a]	**1b** exptl[a]		**3a** exptl[a]	**3a** calcd[a]	**3b** exptl[a]	α-P_4S_5[30] exptl	α-P_4S_5 calcd
$\delta(P_A)$	~113.5[b]	+89	+146.3	$\delta(P_A)$	+173.6	+169	+193.4	+124.9	+117
$\delta(P_B)$	+159.2	+136	+168.6	$\delta(P_B)$	+130.1	+114	+122.2	+91.7	+81
$\delta(P_C)$	~113.5[b]	+167[c]	+44.7	$\delta(P_C)$	+120.0	+190[c]	+62.9	+127.0	+136
$\delta(P_D)$	+257.1	+246	+261.4	$\delta(P_D)$	+266.3	+287	+255.2	+233.8	+242
$\delta(P_E)$	~113.5[b]	+122	+64.1	–	–	–			
$^1J_{A,B}$	–	−215	−191.0	$^1J_{A,B}$	−157.1	−185	−170.4	−184.7	−220
$^2J_{A,C}$	–	+162	+128.7	$^2J_{A,C}$	+164.1	+229	+162.2	+119.0	+149
$^2J_{A,D}$	–	+50	+36.1	$^2J_{A,D}$	+29.8	+31	+27.9	+19.0	+12
$^1J_{A,E}$	–	−257	−206.3	–	–	–			
$^1J_{B,C}$	–	−509	−344.8	$^1J_{B,C}$	−370.9	−490	−342.8	−285.5	−364
$^2J_{B,D}$	–	+86	+74.3	$^2J_{B,D}$	+58.4	+60	+61.6	+53.5	+47
$^2J_{B,E}$	–	−54	+41.6	–	–	–			
$^2J_{C,D}$	–	+55	+54.6	$^2J_{C,D}$	+42.3	+33	+43.7	+27.9	+19
$^1J_{C,E}$	–	−433	−283.2	–	–	–			
$^3J_{D,E}$	–	+44	+28.9	–	–	–			

[a] Labeling of the phosphorus atoms: 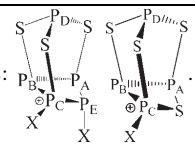 . [b] Three multiplets of **1a** are superimposed in a range of about 18 ppm, centered at about $\delta = 113.5$ ppm. [c] The calculated shifts of these atoms are affected by relativistic effects and are systematically wrong by about +50 to +60 ppm for a P^+–Br moiety.

^{31}P NMR spectroscopic characterization: Prior to discussing the results, it should be noted that we can describe the spin systems by reasonably converged data sets. The standard deviations for the simulation are of the order of 1 Hz. Owing to the sensitivity of the compounds and the unfavorable signal-to-noise ratio, we did not attempt to obtain a higher accuracy of the coupling constants.

*NMR characterization of **1a,b** and **3a,b***: Compound **1b** gives five groups of almost first-order multiplets in the ^{31}P NMR spectrum, in agreement with a C_1-symmetric species, whereas compound **1a** only shows three multiplets at $\delta = +258$, +159, and about +113.5 ppm in a 1:1:3 ratio (see Supporting Information). The signal at $\delta \approx 113.5$ ppm contains three independent signals, thus showing that compound **1a** is also asymmetric. In contrast to the two lines of **1a** at $\delta = 258$ and 159 ppm, this multiplet at $\delta = 113.5$ ppm is of higher order. For **1b**, the simulation with the program WINDAISY was very accurate (see Supporting Information). The proposed assignment of the signals in **1a**,**b** is shown in Table 1, together with the calculated chemical shifts and coupling constants of the $P_5S_3Br_2^+$ ion at the MPW1PW91/6-311G(2df) level. Since we failed to simulate the higher-order spectrum of **1a** adequately, no coupling constants are given for this compound. One should note the similarity of the structures of **1a**,**b** and **3a**,**b** (replace "P(X)" in the four-membered ring of **1a**,**b** by "S" to obtain **3a**,**b**). Accordingly, the chemical shifts and coupling constants of the four equivalent positions in **1a**,**b** and **3a**,**b** are similar. The four signals of **3a** and **3b** were assigned based on the NMR data of α-P_4S_5[30] and the calculated shifts and coupling constants of **3a** and α-P_4S_5.

*NMR characterization of **2a,b**:* Compounds **2a**,**b** give first-order spectra. Since the $P_5S_2X_2^+$ ions are C_s-symmetric, only four groups of signals are observed in the ^{31}P NMR spectrum (Table 2). The signals of the equivalent P atoms in **2a** and **2b** differ by about ±10 to ±25 ppm. The only exception is the P atom of the PX_2^+ unit, with $\delta(^{31}P) = +173.3$ (**2a**) and +61.5 ppm (**2b**). The chemical shift of this phosphonium phosphorus atom is strongly influenced by the inverse halogen dependence that leads to higher frequencies for the heavier halogens.[31] The ^{31}P NMR spectroscopic data of the related neutral P_5S_2X (X = Br, I)[3,4] compounds give similar signal patterns. The only difference is that the neutral species (C_1 symmetry) give five signal groups, since the P_A and P_B atoms are not equivalent (cf. Table 2). Naturally, the greatest differences in the chemical shifts of neutral P_5S_2X compounds are found for the P atoms of the PX unit. The absolute coupling constants $^1J_{E,C}$ and $^1J_{E,D}$ are also about 120 to 230 Hz larger for **2a**,**b** than those of P_5S_2X.

Crystal structures: Compounds **2a**,**b** were characterized by their single-crystal X-ray structures. Compound **2b** crystallized at −28 °C from very concentrated "oily" solutions, whereas the best crystals of **2a** were obtained at room temperature. Crystals of **2b** (**2a**) are air-sensitive, yellow (pale yellow) plates. Since **2a**,**b** represent the same type of structure, the distances and angles of the cations are shown in Table 3 together with the values for the related bonds in P_4S_3 and $P_5Br_2^+$. No other structural data on cationic phosphorus–sulfur cages are available. However, the structures of **2b** (Figure 3) and **2a** can be compared with that of neu-

Table 2. Experimental and MPW1PW91/6-311G(2df) calculated ^{31}P NMR shifts and coupling constants of the cations of **2a** and **2b** in comparison with $P_5X_2^+$ and neutral P_5S_2X (X = Br, I).

	2a exptl[a]	**2a** calcd[a]	**2b** exptl[a]	P_5S_2Br[3] exptl[b]	P_5S_2Br calcd[b]	P_5S_2I[3] exptl[b]		exptl[c]	$P_5Br_2^+$[22,25] exptl[c]	$P_5I_2^+$[22,25]
$\delta(P_A)$	−38.2	−34	−45.7	−70.75	−76	−72.08	$\delta(P_A)$	−237.1	−193.9	
$\delta(P_B)$	−38.2	−34	−45.7	−52.11	−51	−57.33	$\delta(P_B)$	+162.0	+168.2	
$\delta(P_C)$	−292.8	−313	−267.3	−209.11	−224	−200.24	$\delta(P_C)$	+20.0	−89.0	
$\delta(P_D)$	+10.0	+22	+21.0	+30.34	+46	+29.91	$^1J_{A,B}$	−148.7	−152.6	
$\delta(P_E)$	+173.3	+265[d]	+61.5	+169.71	+200[d]	+111.35	$^1J_{A,C}$	25.8	26.7	
$^1J_{A,B}$	–	−212	–	−191.78	−238	−188.58	$^1J_{B,C}$	−320.9	−278.5	
$^1J_{A,C}$	−162.9	−195	−162.3	−169.14	−209	−169.08				
$^2J_{A,D}$	73.6	+77	74.2	73.99	+63	72.75				
$^2J_{A,E}$	13.9	−45	10.5	15.86	+3	17.03				
$^1J_{B,C}$	−162.9	−195	−162.3	−173.51	−214	−168.05				
$^2J_{B,D}$	73.6	+77	74.2	59.45	+57	60.28				
$^2J_{B,E}$	13.9	−45	10.5	−8.67	−23	−8.51				
$^2J_{C,D}$	16.3	−26	−4.4	44.57	+42	45.51				
$^1J_{C,E}$	−616.0	−772	−553.7	−385.97	−463	−368.17				
$^1J_{D,E}$	−416.0	−526	−370.2	−265.21	−323	−251.52				

[a] Labeling of the phosphorus atoms: 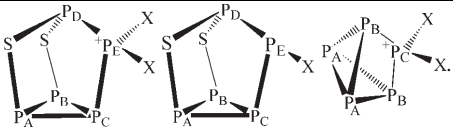

. [b] In CS_2 at 297 K. [c] At 193 K. [d] The calculated shifts of these atoms are affected by relativistic effects and are systematically wrong by about +100 ppm for a P^+Br_2 and about +30 ppm for a P–Br moiety.

Table 3. Important structural parameters of the solid-state structures of the cations of **2a** and **2b** in comparison with the calculated structures and the solid-state structures of P_4S_3 and $P_5Br_2^+$.

Parameter	P_4S_3 exptl		**2a**[a] calcd	**2a** exptl	**2b** exptl	**2b**[a] calcd	$P_5Br_2^+$ exptl
P–P	2.223(1)–2.235(1)	P4–P5	2.253	2.351(6)	2.224(2)	2.251	2.239(8)
$(P–P)_{av}$	2.227(1)	P3–P5	2.253	2.223(6)	2.233(2)	2.251	
		P3–P4	2.226	2.220(5)	2.207(2)	2.229	
P_{ap}–S	2.089(1)–2.098(1)	P2–S2	2.085	2.099(5)	2.075(2)	2.084	
$(P_{ap}–S)_{av}$	2.092(1)	P2–S1	2.085	2.079(5)	2.076(2)	2.084	
P_{bas}–S	2.087(1)–2.089(1)	P3–S1	2.136	2.116(6)	2.115(2)	2.133	
$(P_{bas}–S)_{av}$	2.086(1)	P4–S2	2.136	2.077(6)	2.121(2)	2.133	
		P1–P5	2.178	2.128(5)	2.177(2)	2.182	2.156(7)
		P1–P2	2.227	2.188(5)	2.222(2)	2.233	2.156(7)
		P1–X1	2.155	2.147(3)	2.367(2)	2.376	2.140(3)
		P1–X2	2.155	2.153(4)	2.370(2)	2.376	2.140(3)

[a] Calculated at the MP2/TZVPP level.

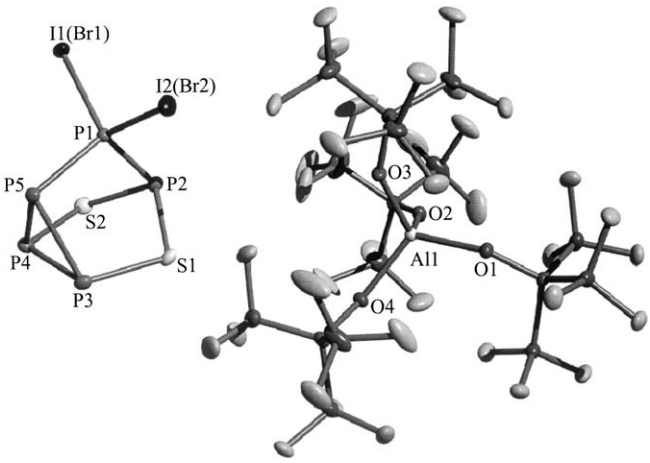

Figure 3. Molecular structure of **2b**. Since **2a** and **2b** are isostructural only **2b** is shown (thermal ellipsoids drawn at the 25% probability level).

tral P_4S_3. The basal P–P bond lengths in **2a**,**b** are in the typical to long range for P–P single bonds (2.207(2) to 2.351(6) Å).[15,22,25] However, the P4–P5 distance in **2a** is longer than other basal P–P bonds in **2a**,**b** or P_4S_3. We attribute this to the bad quality of the crystal and/or crystal packing effects, since this long P–P distance was not reproduced by either BP86/SVP (2.284 Å) or MP2/TZVPP (2.253 Å) calculations. The P–I bonds (2.368(1) Å on average) are equal within the standard deviations and lie in the typical (lower) range for P–I bonds of phosphorus–iodine cations (cf. $P_3I_6^+$: d(P–I) = 2.361(6) to 2.435(6) Å). The P–Br bond lengths (2.150(4) Å, on average) are comparable to those in $P_5Br_2^+$ (2.140(3) Å) and lie in a similar range to the P–Br bond lengths of $P_2Br_5^+$ (2.115(2) to 2.199(3) Å). The two P–P distances around the PX_2 units are shorter towards the P_3 base and differ by 0.045 (X = I) and 0.06 Å (X = Br). The apical P–S bonds in **2a**,**b** are similar to within 0.02 Å, as are the basal P–S bonds to within 0.04 Å. The cage skeleton in **2b** has nearly ideal C_s symmetry, while in **2a** it is more distorted. The formal phosphonium atoms exhibit nearly ideal tetrahedral environments, that is, bond angles of 107.6(2)–111.3(2)° in **2a** and 108.3(1)–111.1(1)° in **2b**.

The structures of the cations in **2a**,**b** were fully reproduced by ab initio MP2 calculations (see Table 3), except for the P4–P5 distance in **2a** (see comment above). The structural parameters of the $[Al(OR)_4]^-$ ion in **2a**,**b** are normal (see Supporting Information).[32]

Using I. D. Brown's empirical formula,[33] we calculated the partial charges residing on the sulfur atoms from the number and lengths of the fluorine contacts shown in Figure 4. The presence and strengths, rather than absence, of contacts is an indication of the higher positive charge residing on the respective atom. The experimentally estimated partial charges or number of contacts, together with the results of population analyses of the calculated structure (MP2 and BP86 level), are summarized in Table 4.

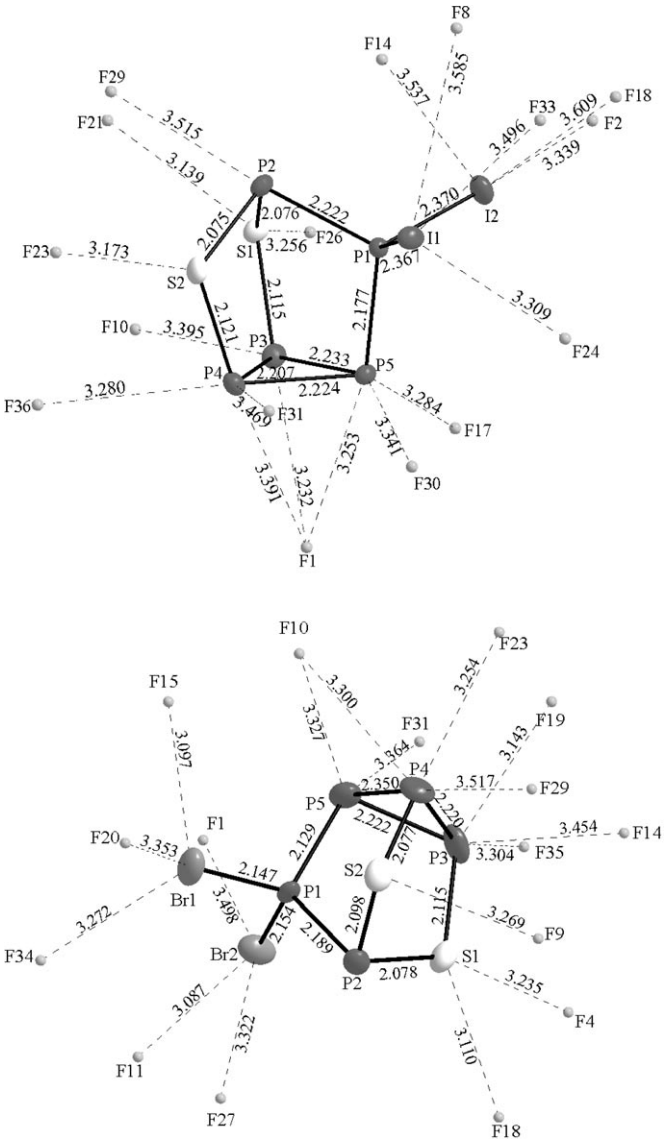

Figure 4. Fluorine contacts [Å] of cation **2b** (top) and **2a** (bottom).

A comparison of the charge distributions obtained by solid-state structure contacts and those calculated at the MP2 or BP86 levels shows that the calculated values are inconsistent with the method and basis set (cf. charges on P1, P5, and Br1/2 above), and the calculated charge-distribution does not agree with the number and strengths of contacts found in the experiment (cf. Table 4 and Figure 4). This failure underlines our earlier finding[16,17] that the charge distributions of ionic species obtained by ab initio or DFT methods are not reliable. If possible, the distribution of the positive charge should be established based on a careful analysis of the solid-state cation–anion contacts.

Table 4. Charge distribution of the cations within the salts **2a** and **2b**.

	2a				**2b**		
atom	exptl charge[a]	MP2 charge[b]	BP/SVP charge[b]	atom	exptl charge[a]	MP2 charge[b]	BP/SVP charge[b]
P1	0 cont.	+0.82	+0.42	P1	0 cont.	+0.50	+0.28
P2	0 cont.	+0.22	+0.18	P2	0 cont.	+0.21	+0.18
P3	3 cont.	+0.16	+0.15	P3	2 cont.	+0.15	+0.15
P4	3 cont.	+0.16	+0.15	P4	3 cont.	+0.15	+0.15
P5	2 cont.	−0.03	+0.06	P5	3 cont.	−0.03	+0.05
S1	+0.13	−0.09	−0.02	S1	+0.13	−0.09	−0.02
S2	+0.06	−0.09	−0.02	S2	+0.13	−0.09	−0.02
Br1	3 cont.	−0.07	+0.05	I1	3 cont.	+0.10	+0.12
Br2	2 cont.	−0.07	+0.05	I2	3 cont.	+0.10	+0.12

[a] cont. = exp. number of fluorine contacts in the solid-state structure. [b] Paboon = population analysis based on occupation numbers.

IR spectroscopy: We recorded the IR spectra of a 1:1 mixture of **2a** and **3a**, as well as pure **2b**. To assign the vibrations of the cations, frequency calculations were carried out at the BP86/SV(P) level. All spectra were simulated by a superposition of Gauss functions using the calculated frequencies and intensities of the cations and the $[Al(OR)_4]^-$ ion, and compared with the experimental as well as a simulated spectrum of the anion (simulations deposited as Supporting Information). The absorptions of all cations appear in the far infrared between 200 and 600 cm^{-1}. The vibrations of **2a** and **2b** are closely related, although the energy of those modes in which halogen atoms are involved differ considerably, for example, $\nu_{as}(X–P–X) = 500\ cm^{-1}$ for **2a** and 427 cm^{-1} for **2b**. In the Raman spectrum of **2b**, the most intense band at 154 cm^{-1} was assigned to the symmetric P_{ap}–PI_2–P_{bas} stretching vibration. The same vibration is found for $P_5I_2^+$ at 168 cm^{-1}. We succeeded in separating and assigning the vibrations of **2a** and **3a** in the 1:1 mixture. The vibrations of the $[Al(OR)_4]^-$ ion were clearly assigned by comparison with known salts (Table 5).

Discussion

The active ingredient of the Ag^+/PX_3 reagent: The reaction of PX_3 (X = Br, I) with $Ag[Al(OR)_4]$[26] in dichloromethane solution at −78 °C may give the electrophilic "PX_2^+" carbene analogue as an intermediate [Eq. (4)] .[16,22,25,27]

$$Ag^+_{(CH_2Cl_2)} + PX_{3(CH_2Cl_2)} \xrightarrow{-78\,^oC} "PX_2{}^+{}_{(CH_2Cl_2)}" + AgX_{(s)} \qquad (4)$$

Despite many attempts, the presence of free PX_2^+ could never be verified experimentally. In contrast, gaseous PX_2^+ has been intensely studied by experimental[34–37] and theoretical means (X = halogen).[38–41] The gas-phase investigations suggested that PX_2^+ may react by insertion into suitable bonds but may also act as a Lewis acid. This also holds for other "PR_2^+" reagents in condensed phases (see, for example, the insertion and/or coordination chemistry of the "R_2P^+" reagents R_2PCl/Me_3SiOTf or $R_2PCl/GaCl_3$ observed by Burford et al.[42–46]).

Table 5. Experimental IR/Raman (RA) bands of **2a**,**b** and **3a**. Tentative assignment of the cation vibrations. The IR/Raman frequencies of the $[Al(OR)]_4^-$ ion are compared to those of $CS_2Br_3^+[Al(OR)]_4^-$.[17] The bands and assignments of the cations are given in italics.

3a assignment	**3a** calcd [km mol^{-1}]	**3a** and **2a** IR	**2a** calc	**2a** assignment	**2b** IR	**2b** Raman [%]	**2b** calcd [km mol^{-1}]	**2b** assignment	$[Al(OR)_4]^-$
			53(0)				42(0)		
	68(0)		*57(0)*				49(0)		
	94(0)		*94(1)*				63(1)		
	142(0)		*110(1)*			*110(5)*	*93(1)*		
	150(1)		*151(0)*	$\nu_s(P_{ap}–PX_2–P_{bas})$		*147(sh)*	*130(1)*		
	173(0)		*169(0)*			*154(100)*	*135(0)*	$\nu_s(P_{ap}–PX_2–P_{bas})$	
	207(2)		*176(1)*			*187(5)*	*174(1)*		
		216(w)			215(w)	214(10)			IR: 215(w); RA: 216(5)
		230(vw)	*203(5)*	$\delta_s(P_{ap}–S_2)$	*229(w)*		*202(7)*	$\delta_s(P_{ap}–S_2)$	
						230(10)			RA: 232(5)
						245(5)			RA: 245(5)
$\delta_s(P_{ap}–S_2)$	*214(3)*	*235(vw)*							
		285(m)			286(w)				284(w)
	221(2)		*273(0)*						
						260(10)	*269(15)*	$\delta(S_2–P_{ap}–PX_2)$	
			278(7)		*290(m)*	*288(65)*	*273(0)*		
	264(2)								
	301(2)								
	310(1)								
		315(s)			315(m)				314(w)
		331(w)			331(w)	320(70)			IR: 330(vw); RA: 318(sh)
		346(m)	*323(11)*	$\nu(S_2–P_{ap}–PX_2)$	*335(m)*		*317(19)*	$\nu_s(S_2–P_{ap}–PX_2)$	
			327(2)			*336(40)*	*324(4)*		
	329(1)								
			333(4)			*345(sh)*	*333(3)*		
	347(5)								
					372(w)	361(20)			365–427(br)
$\nu(BrP_{bas}–P_{bas})$	*358(17)*	*375(m)*							
$\nu_s(S–P_{ap}–S)$	*370(21)*	*392(vs)*	*367(4)*		*404(m)*	*368(15)*	*365(10)*	$\nu_s(X_2P–P_{ap})$	
$\nu_{as}(P_{bas}–S_{ap}–P_{ap})$	*390(17)*	*409(s)*				*411(20)*	*366(7)*	$\nu_s(X–P–X)$	
			386(4)						
		422(m)	*419(17)*	$\nu_s(X–P–X)$	*427(s)*	*420(sh)*	*384(58)*	$\nu_{as}(X–P–X)$	
$\nu_s(P_{bas}–S_{ap}–P_{ap})$	*427(10)*	*437(s)*			*436(sh)*		*391(10)*	$\nu_{as}(P_{bas}–S_2)$	
					442(sh)	*443(10)*	*423(12)*	$\nu(X_2P–P_{bas})$	
			432(2)			*459(20)*	*433(18)*	$\nu_s(S–P_{ap}–S)$	
		444(s)			444(s)				445(m)
		489(m)	*448(19)*	$\nu_{as}(P_{ap}–S_2)$					
			450(73)	$\nu(X_2P–P_{bas})$					
$\nu_{as}(P_{bas}–P_{bas}–Br)$	*464(37)*	*500(m)*	*467(53)*	$\nu_{as}(X–P–X)$	*483(m)*	*480(5)*	*458(8)*	$\nu_{as}(P_{ap}–S_2)$	
			468(1)		*491(w)*		*465(4)*	$\nu_s(P_3)$	
$\nu_{as}(Br–P_{bas}–S_{ap})$	*484(51)*	*518(m)*							
$\nu(P_{bas}–S_{ap})$	*494(26)*	*528(m)*							
		536(s)			536(s)				537(mw)
		561(s)			561(m)				561(mw)
		571(m)			571(m)				571(w)
$\nu_{as}(S_{bas}–P_{bas}–S_{ap})$	*542(40)*	*589(m)*							
		638(w)							$[(RO)_3AlFAl(OR)_3)]^-$
		728(s)			727(vs)				728(s)
						745(10)			RA: 745(20)
		756(m)			755(m)				755(w)
						796(10)			RA: 797(20)
		831(m)			831(m)				832(m)
		863(w)							$[(RO)_3AlFAl(OR)_3)]^-$
		976(vs)			972(vs)				973(vs)
					1079(w)				1075(sh)
		1136(s)							1133(sh)
		1161(s)			1161(w)				1169(ms)
		1220(s)			1219(vs)				1219(vs)

Table 5. (Continued)

3a assignment	**3a** calcd [km mol^{-1}]	**3a** and **2a** IR	**2a** calc	**2a** assignment	**2b** IR	**2b** Raman [%]	**2b** calcd [km mol^{-1}]	**2b** assignment	$[Al(OR)_4]^-$
		1247(vs)			1247(vs)				1242(vs)
		1264(s)							
		1277(s)			1275(vs)				1276(vs)
		1299(s)			1299(vs)				1301(s)
		1353(m)			1353(s)				1353(ms)

The Ag^+/PX_3 ("PX_2^+") reagent prepared according to Equation (4) reacts with the bonds of a limited set of substrates in a way that suggests insertion is preferred over coordination. This likely insertion is most evident for P_4 as a substrate (to give $P_5X_2^+$).[22,25] Only one type of bond is available for the proposed insertion with P_4, PX_3, and X_2 as a substrate. Moreover, it is not possible to distinguish between "PX_2^+" insertion and "PX_2^+" coordination with the substrates PX_3 and P_2I_4.[47] Therefore, we were interested in extending this chemistry to substrates with a limited number of different bonds that, upon insertion or coordination of "PX_2^+", would remain intact as such, for example P_4S_3, with the hope of gaining an insight into the electronic preference of the proposed "PX_2^+" intermediate.

Quantum-chemical calculations suggested that P-coordination as well as P–P insertion should be thermodynamically favored over S-coordination and P–S insertion (by +15 to +61 kJ mol^{-1}, MP2/TZVPP). However, none of the six isomers given in Figure 5 fitted well with the experimental NMR spectroscopic data of **1a**,**b**. The calculation of the chemical shifts and the P–P coupling constants for all six isomers (see Supporting Information) supports this conclusion, and shows that the Ag^+/PX_3 reagent shows a different type of reactivity to coordination or insertion towards the P_4S_3 cage. The finally assigned structure of **1a**,**b** (Figure 6) shows the P–X disruptive addition of PX_2^+ towards the P_4S_3 cage. It is the global minimum of all the $P_5S_3X_2^+$ structures assessed so far and is lower in energy than all the other isomers shown in Figure 5 by 14 (Br) and 16 (I) kJ mol^{-1}.

Compounds **1a** and **1b** were the first species to be identified in low temperature in situ NMR reactions kept at −78 °C. Therefore, a concerted addition of the "PX_2^+" intermediate to P_4S_3 appeared likely. The most likely scenario for such a concerted addition would involve the frontier orbitals of "PX_2^+" and P_4S_3. The respective HOMO and LUMO orbital energies are collected in Table 6.

From an inspection of these orbital energies it is clear that the most likely interaction involves the HOMO of P_4S_3 and the LUMO of PX_2^+. However, the LUMO of PX_2^+ has π* symmetry and coefficients on all three atoms. For this reason one would expect a different reactivity for this free PX_2^+ than is observed with P_4S_3. This rendered the presence of the free PX_2^+ cation in solution unlikely.

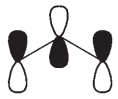

We have recently shown computationally that Ag^+ and PX_3 form complexes in CH_2Cl_2 solution that can be considered as intermediates on the way to the formation of PX_4^+ and $P_2X_5^+$.[16,27] Thus, it appeared likely that the true "PX_2^+" reagent is in fact a mixed $Ag–CH_2Cl_2–PX_3$ complex. We therefore analyzed the possibility that $[(CH_2Cl_2)Ag(PBr_3)]^+$ acts as a PBr_2^+ source by performing DFT calculations. All three isomers shown in Figure 7 lie within 8 kJ mol^{-1} of each other and are therefore in rapid exchange (BP86/SVP, free energies in CH_2Cl_2 solution).

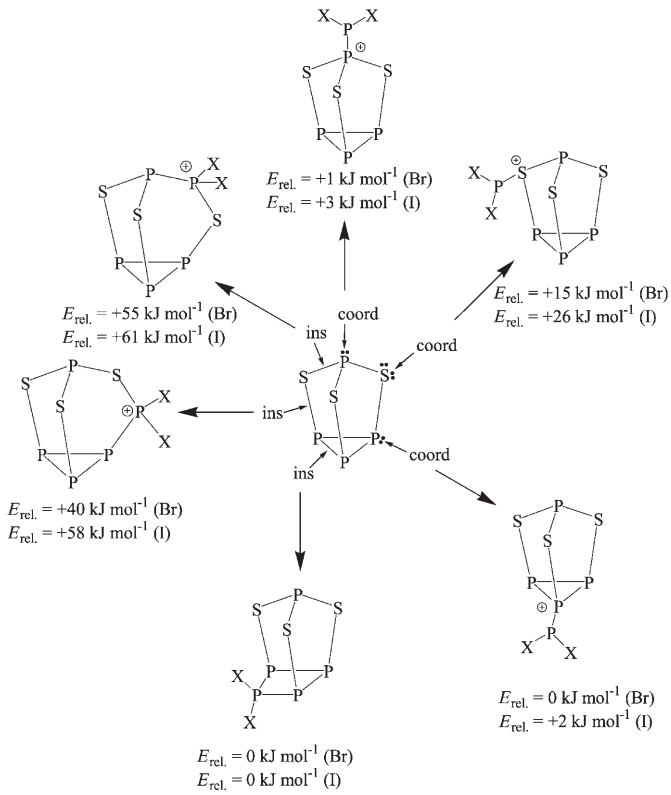

Figure 5. The six likely sites of "PX_2^+" attack and the resulting products, with their relative free-energies, in CH_2Cl_2 solution at 298 K (MP2/TZVPP).

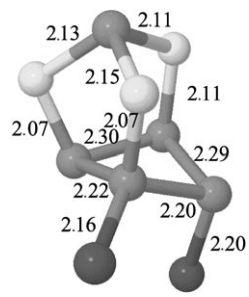

Figure 6. The optimized structure of the cation in **1a** (MP2/TZVPP, distances in Å).

Table 6. HOMO and LUMO orbital energies of PBr_2^+, PI_2^+, and P_4S_3 (HF/TZVPP).

	P_4S_3	PBr_2^+	PI_2^+
HOMO	−0.348 H	−0.632 H	−0.571 H
	(−9.471 eV)	(−17.192 eV)	(−15.530 eV)
LUMO	+0.047 H	−0.264 H	−0.255 H
	(+1.291 eV)	(−7.187 eV)	(−6.952 eV)

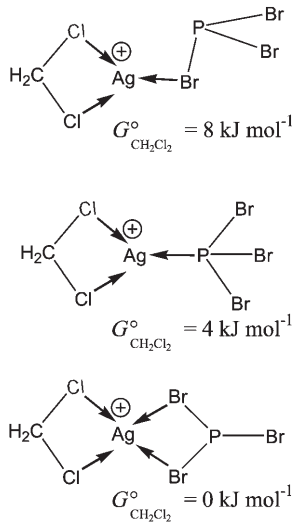

Figure 7. The relative free energies of three $(CH_2Cl_2)Ag(PBr_3)^+$ isomers in CH_2Cl_2 solution.

Since the coordinated P–Br distance in the monodentate complex is elongated to 2.39 Å and the Ag–Br distance is as short as 2.54 Å, the structure with a monodentate Br-PBr_2 moiety is closest to being a "PBr_2^+" intermediate. These distances should be compared to those in free PBr_3 (2.27 Å) and free AgBr (2.42 Å) at the same level. Thus, the CH_2Cl_2–Ag–Br-PBr_2^+ complex is halfway towards ionization and formation of PBr_2^+ and AgBr. An inspection of the energies and nature of the frontier orbitals revealed that the LUMO of CH_2Cl_2–Ag–Br-PBr_2^+ has only coefficients at the P and two of the three Br atoms. This frontier orbital is well suited for a concerted and P–X disruptive interaction with the HOMO of P_4S_3 (Figure 8).

In this process, electron density from the occupied P_4S_3 HOMO is transferred into the LUMO of CH_2Cl_2–Ag–Br-PBr_2^+, which is antibonding with respect to two of the three P–X moieties. Consequently, such an interaction would facilitate cleavage of $(CH_2Cl_2)AgBr$ and also lead to a P–X-disruptive addition of a PX_2^+ moiety to P_4S_3, as observed by NMR spectroscopy. Therefore, we propose that the active ingredient of the Ag^+/PX_3 reagent in CH_2Cl_2 solution is the monodentate complex $(CH_2Cl_2)Ag$–Br-PBr_2^+.

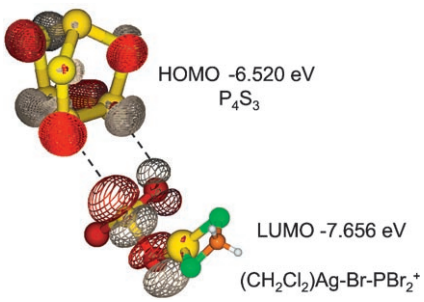

Figure 8. Possible concerted interaction of P_4S_3 (HOMO) with CH_2Cl_2Ag–Br-PBr_2^+ (LUMO; Kohn–Sham orbitals at BP86/SVP).

On the formation of $P_5S_3X_2^+$ 1a,b: Based on the available experimental data and the above conclusions we propose the following mechanism for the formation of **1a**,**b** (Figure 9).

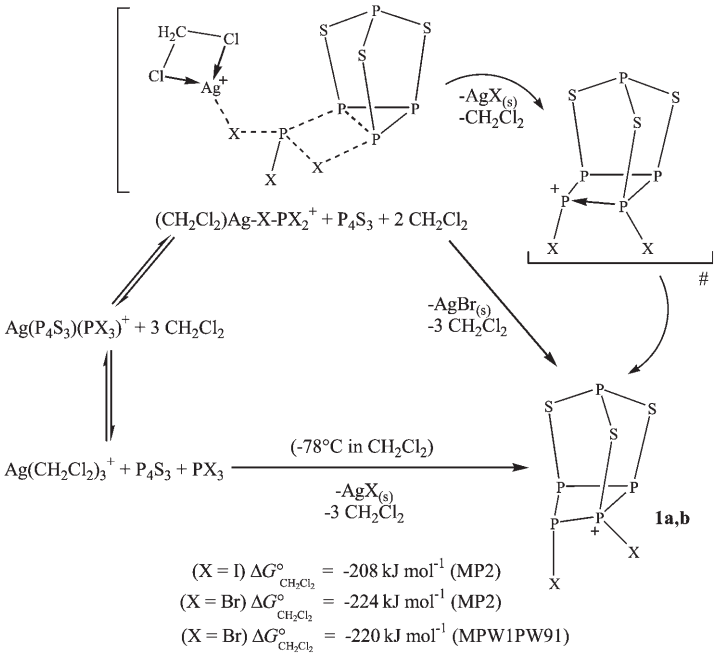

Figure 9. Likely mechanism for the formation of **1a** (as well as **1b**).

The formation of the proposed $Ag(P_4S_3)(PBr_3)^+$ complexes is likely and favorable in CH_2Cl_2 solution by −11 to −22 kJ mol^{-1} ($\Delta G°_{CH_2Cl_2}$; nine isomers assessed at the BP86/SVP level; see Supporting Information). The similarity of the relative energies of the nine isomers also gives an explanation for the broad lines in the NMR spectrum of the reaction mixture: all complexes are in dynamic exchange, which leads to line broadening, and the chemical shifts of the ligands PBr_3 and P_4S_3 are only slightly different to those of the free molecules. From these $Ag(P_4S_3)(PBr_3)^+$ complexes, it is likely that $(CH_2Cl_2)Ag$–BrPBr_2^+ and P_4S_3 form as intermediates, which react by the above-mentioned concerted HOMO–LUMO interaction to give **1a**,**b**. The entire reaction is highly exergonic by −208 to −224 kJ mol^{-1} for **1a**,**b**, respectively.

The disproportionation of $P_5S_3X_2^+$: Formation of $P_5S_2X_2^+$ and $P_4S_4X^+$: Once the formation of **1a**,**b** is complete at −78 °C, they disproportionate at higher temperature into the products $P_5S_2X_2^+$ (**2a**,**b**), $P_4S_4X^+$ (**3a**,**b**), and a species we

have tentatively assigned as $(PX)_6$, thereby recovering the nortricyclane skeleton in **2a**,**b**. For $1/n(PI)_n$ (such as P_6I_6, P_4I_4, or P_2I_2), no signals were observed that could be assigned unequivocally. The sharp singlet in the spectrum of a crystalline mixture of **2a** and **3a** at $\delta = +228$ ppm may be assigned to PBr_3 ($\delta(CH_2Cl_2) = +228$ ppm) or P_6Br_6 (δ-(THF) $= +220$ ppm).[48] However, P_6Br_6 is known to be only stable for a few hours in dilute solution and its decomposition products always contain PBr_3. Thus, the assignment is not clear. The ^{31}P NMR signals of the identified products (**2a**,**b** and **3a**,**b**) grow at the same time as the signals of **1a**,**b** disappear. Therefore, it is highly possible that **2a** and **3a** (**2b** and **3b**) result from a collision of two **1a** (**1b**) cations with formation of P_2X_2, which subsequently and irreversibly polymerizes to give $(PX)_6$. This thesis is supported by the calculated thermodynamics [Eq. (5)].

$$2P_5S_3X_2^{+}{}_{(solv.)} \longrightarrow P_5S_2X_2^{+}{}_{(solv.)} + P_4S_4X^{+}{}_{(solv.)} + 1/6\ P_6X_{6(solv.)} \qquad (5)$$

MP2	MP2 (MPW1PW91)
X = I: $\Delta G^{\circ}_{(CH_2Cl_2)} = -10.2$ kJ mol^{-1}	X = Br: $\Delta G^{\circ}_{(CH_2Cl_2)} = -12.5$ (-4.1) kJ mol^{-1}
$\Delta G^{243K}_{(CH_2Cl_2)} = -9.6$ kJ mol^{-1}	$\Delta G^{243K}_{(CH_2Cl_2)} = -11.6$ (-1.1) kJ mol^{-1}
$\Delta G^{193K}_{(CH_2Cl_2)} = -8.9$ kJ mol^{-1}	$\Delta G^{193K}_{(CH_2Cl_2)} = -10.7$ (0.2) kJ mol^{-1}

In agreement with the experiment, the disproportionation reaction shown in Equation (5) is slightly exergonic at room temperature and less favorable at low temperature. This accounts for the observed metastable formation of **1a**,**b** at −78 °C.

The MP2/TZVPP-optimized structures of **2a**,**b** were included with the X-ray data above; those of the cations in **3a**,**b** are shown in Figure 10.

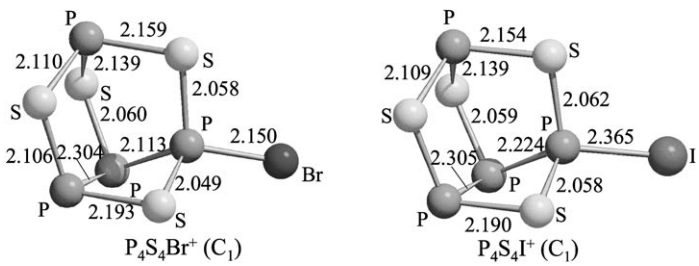

Figure 10. MP2/TZVPP-optimized structures of the cations in **3a**,**b**.

Conclusion

The current contribution suggests that the "PX_2^+" intermediate generated from PX_3 and $Ag[Al(OR)_4]$ is likely to be $(CH_2Cl_2)Ag–X–PX_2^+$. The initially assumed insertion or coordination of the "PX_2^+" intermediate was not observed; rather, this Ag^+/PX_3 mixture may react in a concerted manner with P_4S_3 to give the $P_5S_3X_2^+$ ions **1a**,**b**, which are metastable at −78 °C. Above −78 °C, these cations disproportionate intermolecularly into the cations $P_5S_2X_2^+$ (**2a**,**b**) and $P_4S_4X^+$ (**3a**,**b**). Cations **2a**,**b** have been characterized by their X-ray crystal structures and represent the first structurally characterized examples of any ternary P–Ch–X cation (Ch = O–Te, X = F–I).

The Ag^+/PX_3 reagents appears to be a selective "PX_2^+" equivalent (X = Br, I) that allows the introduction of a PX_2^+ moiety to a given substrate, especially P_4S_3, P_4, P_2I_4, PX_3, and X_2. Owing to the different frontier orbitals of free PX_2^+ and $(CH_2Cl_2)Ag–X–PX_2^+$, its reactivity may be markedly different to the chemistry of the free PX_2^+ ion, which is as-yet unknown in the condensed phase.

Experimental Section

General: All manipulations were performed by using standard Schlenk or dry-box techniques under dinitrogen or argon (H_2O and $O_2 < 1$ ppm). Reaction vessels were closed by J. Young valves with a glass stem (leak-tight at −80 °C). All solvents were rigorously dried over P_2O_5, degassed prior to use, and stored under N_2. PBr_3 (Fluka), I_2 (Merck), and P_4S_3 (Aldrich) were purchased and purified prior to use by distillation, sublimation, and recrystallisation from CS_2. PI_3 was prepared from white phosphorus and iodine in CS_2 and its purity was checked by Raman spectroscopy. $M[Al(OR)_4]$ (M = Li, Ag) was prepared according to the literature.[24,26] Raman and IR spectra were recorded using a 1064-nm laser on a Bruker IFS 66v spectrometer equipped with the Raman module FRA106. IR spectra were recorded from Nujol mulls between CsI plates. NMR spectra of sealed samples were recorded on a Bruker AC250 spectrometer in CD_2Cl_2 and are referenced to the solvent (^1H, ^{13}C) or external H_3PO_4 (^{31}P), $CFCl_3$ (^{19}F), or aqueous $AlCl_3$ (^{27}Al). The ^{31}P NMR spectra were simulated and assigned with the programs WINNMR and WINDAISY.[49]

Synthesis of $P_5S_3Br_2^+[Al(OR)_4]^-$, $P_4S_4Br^+[Al(OR)_4]^-$, and $P_5S_2Br_2^+[Al(OR)_4]^-$

Synthesis of $P_5S_3Br_2^+[Al(OR)_4]^-$, NMR-tube reaction: $Ag[Al(OR)_4]$ (0.495 g, 0.427 mmol) and P_4S_3 (0.094 g,0.427 mmol) were weighed under inert atmosphere into an NMR tube attached to a valve. CD_2Cl_2 (0.8 mL) was condensed onto the solids at −78 °C and then PBr_3 (0.115 g, 0.040 mL, 0.427 mmol) was added with a 50-μL Hamilton syringe fitted with a Teflon needle. Precipitation of AgBr occurred immediately. The NMR tube was sealed under vacuum at −196 °C and kept at −78 °C until the spectrum was recorded. The ^{31}P NMR spectra showed three groups of signals (in a 1:1:3 ratio), which were assigned to $P_5S_3Br_2^+[Al(OR)_4]^-$ as well as the unreacted substrates PBr_3 and P_4S_3 involved in the exchange processes. (original spectrum available as Supporting Information).

^{31}P NMR (101 MHz, CD_2Cl_2, −70 °C): $P_5S_3Br_2^+$: $\delta = 257.1$ (m, 1P), 160.5 (m, 1P), 116.0 ppm (m, 3P); PBr_3: $\delta = 225.6$ (br. s, $\nu_{1/2} = 960$ Hz); P_4S_3: $\delta = 87.9$ (br. s, $\nu_{1/2} = 470$ Hz), −105.7 ppm (br. d, $J = 1661.6$ Hz, $\nu_{1/2} = 726$ Hz). ^{13}C NMR (63 MHz, CD_2Cl_2, −70 °C): $\delta = 120.6$ (q, $J_{C,F} = 292.4$ Hz, CF_3), 79.0 (m, $C_{tert}(CF_3)_3$). ^{27}Al NMR (78 MHz, CD_2Cl_2, −50 °C): $\delta = 38.3$ ppm (s, $\nu_{1/2} = 86.0$ Hz).

Synthesis of $P_5S_2Br_2^+[Al(OR)_4]^-$: $Ag[Al(OR)_4]$ (0.679 g, 0.585 mmol) and P_4S_3 (0.129 g, 0.585 mmol) were transferred under an inert atmosphere into a two-bulb vessel incorporating a sintered glass frit and closed by Young valves with a glass stem. CH_2Cl_2 (10 mL) was added, the resulting mixture was cooled to −78 °C, and PBr_3 (0.158 g, 0.056 mL, 0.585 mmol) was then added with a Hamilton syringe. The reaction mixture was kept at −78 °C until AgBr had precipitated almost quantitatively. The flask was left for an additional two days at −28 °C and after that time some more solid AgBr appeared. The solution was filtered from the precipitate, concentrated, and left to crystallize at −25 °C. No crystals appeared after 2–3 weeks of storage, therefore the solution was further concentrated until it formed an oily, viscous, and turbid phase. Very pale-yellow crystals of $P_5S_2Br_2^+[Al(OR)_4]^-$ grew from this oily phase after

one day at room temperature (yield: 0.187 g, 24%). These crystals were used for the crystal-structure determination and NMR and vibrational spectroscopy.

Synthesis of a 1:1 mixture of $P_5S_2Br_2^+[Al(OR)_4]^-$ and $P_4S_4Br^+[Al(OR)_4]^-$: This compound was synthesized from $Ag[Al(OR)_4]$ (1.000 g, 0.862 mmol), P_4S_3 (0.189 g, 0.862 mmol), and PBr_3 (0.233 g, 0.082 mL, 0.862 mmol) in a manner similar to the synthesis of $P_5S_2Br_2^+[Al(OR)_4]^-$, except that, to increase the rate of transformation, the flask was kept for about 24 h at 0°C. After this period of time the solution was filtered from the yellowish precipitate, concentrated to about one quarter the original volume, and stored at −25°C. Crystalline solids precipitated quantitatively and the solvent was decanted and removed in vacuo. Samples for NMR and IR spectroscopy were prepared from this crystalline material.

^{13}C NMR (63 MHz, CD_2Cl_2, −30°C): $\delta = 121.0$ (q, $J_{C,F} = 291.3$ Hz, CF_3, undecomposed anion), 120.5 ppm (q, $J_{C,F} = 292.1$ Hz, CF_3, decomposition product, probably $[(RO)_3Al\text{-}F\text{-}Al(OR)_3]_4^-$, accounting for about 20% of the intensity of the main signal)

Synthesis of $P_5S_3I_2^+[Al(OR)_4]^-$, $P_4S_4I^+[Al(OR)_4]^-$, and $P_5S_2I_2^+[Al(OR)_4]^-$

NMR-scale synthesis of $P_5S_3I_2^+[Al(OR)_4]^-$: $Ag[Al(OR)_4]$ (0.120 g, 0.112 mmol), P_4S_3 (0.025 g, 0.112 mmol), and PI_3 (0.046 g, 0.112 mmol) were loaded, in a glove box, into an NMR tube attached to a valve. CD_2Cl_2 (0.8 mL) was then condensed onto the mixture at −78°C. The immediate precipitation of a yellow solid (AgI) was observed. The NMR tube was then sealed and stored at −80°C until the spectrum was measured (16 h). Shortly before the measurement the sample was shaken and warmed for one minute to about −30°C. The sample was measured at different temperatures (Figure 2). After every measurement, the sample was shaken at ambient temperature for about 20–30 s so that the reaction proceeded. ^{31}P NMR data of **1b**, **2b**, and **3b** are given in the NMR section above. Additional NMR data: ^{13}C NMR (63 MHz, CD_2Cl_2, −70°C): $\delta = 120.5$ ppm (q, $J_{C,F} = 292.1$ Hz, CF_3). ^{27}Al NMR (78 MHz, CD_2Cl_2, −30°C): $\delta = 37.5$ ppm (s, $\nu_{1/2} = 35.0$ Hz).

Large-scale synthesis of $P_5S_2I_2^+[Al(OR)_4]^-$: $Ag[Al(OR)_4]$ (0.500 g, 0.431 mmol), P_4S_3 (0.177 g, 0.431 mmol), and PI_3 (0.095 g, 0.431 mmol) were loaded in a glove box into a two-bulb vessel closed by Young valves and CH_2Cl_2 (10 mL) was condensed onto the mixture at −78°C. Immediate precipitation of a yellow solid (AgI) was observed. The flask was occasionally shaken and kept at −78°C until the reaction was finished (no new formation of AgI visible). The yellow solution was filtered from the solids and concentrated to about one quarter. Yellow crystals of $P_5S_2I_2^+[Al(OR)_4]^-$ grew from the concentrated solution after 1–2 weeks at −30°C (yield of crystalline material: 0.252 g, 41% with respect to $Ag[Al(OR)_4]$).

^{13}C NMR (63 MHz, CD_2Cl_2, −30°C): $\delta = 121.1$ ppm (q, $J_{C,F} = 293.2$ Hz, CF_3). ^{27}Al NMR (78 MHz, CD_2Cl_2, −30°C): $\delta = 37.5$ ppm (s, $\nu_{1/2} = 47.0$ Hz).

X-ray crystal structure determinations: Data collection for X-ray structure determinations was performed on a STOE IPDS II diffractometer using graphite-monochromated $Mo_{K\alpha}$ ($\lambda = 0.71073$ Å) radiation. Crystals were mounted in perfluoroether oil on top of a glass fiber and then placed in the cold stream of a low-temperature device so that the oil solidified. All calculations were performed on a PC using the SHELX97 software package. The structures were solved by direct methods and successive interpretation of the difference Fourier maps, followed by least-squares refinement (see Table 7). The crystal structure of **2a** which, according to the cell parameters is orthorhombic, was refined as a monoclinic twin ($\beta = 90.05(3)°$) with the yz mirror plane being the twin element (transformation matrix: −100, 010, 001). Nevertheless, the agreement factors are not satisfactory due to additional heavy disorder. All the $C(CF_3)_3$ groups in **2a** had to be fixed with SADI restraints. Due to the similarity of the cell parameters of **2a** and **2b** and the agreement with the MP2 calculation, we have taken the structure of **2a** as a structural proof for the formation of **2a** but resist discussing the structural parameters in depth. All the $C(CF_3)_3$ groups in the anion of **2b** were also fixed with SADI restraints and six CF_3 moieties of two $C(CF_3)_3$ groups had to be (partially) split over two positions (70% main occupation); they were included anisotropically in the refinement.CCDC-259932 (**2a**) and CCDC-259933 (**2b**) contain the supplementary crystallographic data for this paper. These data can be obtained free of charge from the Cambridge Crystallographic Data Centre via www.ccdc.cam.ac.uk/data_request/cif.

Table 7. Crystallographic details for $P_5S_2Br_2^+[Al(OR)_4]^-$ (**2a**) and $P_5S_2I_2^+[Al(OR)_4]^-$ (**2b**).

	2a	**2b**
crystal size [mm^3]	0.3×0.2×0.1	0.6×0.3×0.1
crystal system	monoclinic	monoclinic
space group	$P2_1/n$	$P2_1/c$
a [Å]	13.776(3)	13.739(3)
b [Å]	19.355(4)	14.514(3)
c [Å]	14.446(3)	19.715(4)
α [°]	90.000	90
β [°]	90.05(3)	91.78(3)
γ [°]	90.000	90
V [Å^3]	3851.9(13)	3929.3(1)
Z	4	4
ρ_{calcd} [Mg m^{-3}]	2.321	2.434
μ [mm^{-1}]	2.649	2.135
max./min. trans.	0.5250/0.6261	0.3596/0.4992
index range	$-16 \le h \le 16$	$-17 \le h \le 17$
	$-20 \le k \le 22$	$-18 \le k \le 18$
	$-17 \le l \le 14$	$-24 \le l \le 25$
2θ [°]	52.0	54.3
temperature [K]	130	120
refl. collected	22213	37150
refl. unique	20504	8612
refl. observed (2σ)	8308	8109
R(int.)	0.238	0.0646
GOOF/GOOF restrained	1.109/1.108	1.183/1.189
final $R/wR2$ (2σ)	0.1580/0.3642	0.0424/0.1001
final $R/wR2$ (all data)	0.2748/0.4369	0.0446/0.1011
larg. res. peak [e Å^{-3}]	1.992	0.799

Computational details: The majority of the calculations were performed with the program TURBOMOLE.[50,51] The geometries of all species were optimized at the (RI-)MP2 level[52] with the triple ζ valence polarization TZVPP basis set (one f and two d functions).[53,54] The 28- and 46-electron-cores of Ag and I were replaced by a quasi-relativistic effective core potential.[55] All species were also fully optimized at the (RI-)BP86/SV(P) (DFT−)level. Approximate solvation energies [CH_2Cl_2 solution with $\varepsilon_r = 8.93$ (298 K), 11.46 (243 K), and 14.95 (195 K)] were calculated with the COSMO model[56] at the (RI-)BP86/SV(P) (DFT−)level. Frequency calculations were performed for all species, and the structures represent true minima without imaginary frequencies on the respective hypersurface. For thermodynamic calculations the zero-point energy and thermal contributions to the enthalpy and the free energy at 298 K (and for some species at 243 and 195 K) were included. The calculation of the thermal contributions to the enthalpy and entropic contributions to the free energy were done with TURBOMOLE using the FreeH module. For some species a modified Roby–Davidson population analysis based on occupation numbers (paboon) was performed using the (RI-)MP2/TZVPP electron density. The calculation of the chemical shifts and the spin–spin J-coupling constants was done with Gaussian 03 at the MPW1PW91/6-311G(2df) level of theory (keyword nmr=spinspin) with fully optimized structures obtained at the same level.[57] The MPW1PW91/6-311G(2df) level was selected since it also reproduces quantum chemical problem cases like the S_4^{2+} and S_8^{2+} cations.[58–60] The referencing of the calculated chemical shifts was done in analogy to the procedure described by Tattershall,[3] with the only difference being that all halogen-bearing atoms, which are known to be systematically in error due to relativistic effects,[31] were omitted for the assignment of the reference values. The reference value for $\delta_{^{31}P} = 0$ ppm for $P_5S_3Br_2^+$ was 276.2 ppm, for $P_5S_2Br_2^+$ it was 318.4 ppm, for P_5S_2Br it was 323.6 ppm, for $P_4S_4Br^+$ it was 296.0 ppm, and for P_4S_5 it was 301.2 ppm for the abso-

lute isotropic shielding tensor. All calculated chemical shifts and coupling constants, together with machine readable *xyz*-orientations of the calculated structures and the calculated vibrational frequencies, are given as Supporting Information.

Acknowledgements

This work was supported by the Deutsche Forschungsgemeinschaft, the Fonds der Chemischen Industrie, the Universität Karlsruhe, and the EPFL. We would like to thank Dr. J. Sawatzki of the Bruker demonstration lab for recording the Raman spectrum. We are grateful to Prof. M. Kaupp, Dr. J. Slattery and Prof. H. Schnöckel for many useful discussions. Moreover, we have to thank one of the referees who spotted the erroneous assignment of our initial structures of **1a**,**b**.

[1] N. N. Greenwood, A. Earnshaw, *Chemistry of Elements*, Butterworth–Heinemann, Oxford, **1997**.
[2] A. Frehn, H. Keck, W. Kuchen, *Chem. Ber.* **1990**, *123*, 1335–1337.
[3] B. W. Tattershall, R. Blachnik, A. Hepp, *J. Chem. Soc. Dalton Trans.* **2000**, 2551–2558.
[4] B. W. Tattershall, N. L. Kendall, *Polyhedron* **1994**, *13*, 2629–2637.
[5] R. Blachnik, G. Kurz, U. Wickel, *Z. Naturforsch., Teil B* **1984**, *39*, 778–782.
[6] G. M. Sheldrick, G. J. Penney, *J. Chem. Soc. A* **1971**, 1100–1103.
[7] A. W. Cordes, G. W. Hunt, *Inorg. Chem.* **1971**, *10*, 1935–1938.
[8] M. Baudler, H. W. Valpertz, K. Kipker, *Chem. Ber.* **1967**, *100*, 1766–1767.
[9] O. J. Scherer, *Acc. Chem. Res.* **1999**, *32*, 751–762.
[10] H. G. Von Schnering, W. Hönle, *Chem. Rev.* **1988**, *88*, 243–273.
[11] M. Baudler, *Phosphorus Sulfur Relat. Elem.* **1987**, *30*, 345–348.
[12] M. Baudler, *Angew. Chem.* **1987**, *99*, 429–451; *Angew. Chem. Int. Ed. Engl.* **1987**, *26*, 419–441..
[13] W. Dahlmann, H. G. Von Schnering, *Naturwissenschaften* **1972**, *59*, 420.
[14] B. H. Christian, R. J. Gillespie, J. F. Sawyer, *Inorg. Chem.* **1981**, *20*, 3410–3420.
[15] I. Krossing, *J. Chem. Soc. Dalton Trans.* **2002**, 500–512.
[16] M. Gonsior, I. Krossing, *Dalton Trans.* **2005**, 1203–1213.
[17] M. Gonsior, I. Krossing, *Chem. Eur. J.* **2004**, *10*, 5730–5736.
[18] I. Krossing, I. Raabe, *Chem. Eur. J.* **2004**, *10*, 5017–5030.
[19] I. Krossing, I. Raabe, *Angew. Chem.* **2004**, *116*, 2116–2142; *Angew. Chem. Int. Ed.* **2004**, *43*, 2066–2090.
[20] I. Krossing, A. Reisinger, *Angew. Chem.* **2003**, *115*, 5903–5906; *Angew. Chem. Int. Ed.* **2003**, *42*, 5725–5728.
[21] I. Krossing, A. Bihlmeier, I. Raabe, N. Trapp, *Angew. Chem.* **2003**, *115*, 1569–1572; *Angew. Chem. Int. Ed.* **2003**, *42*, 1531–1534.
[22] M. Gonsior, I. Krossing, L. Müller, I. Raabe, M. Jansen, L. Van Wüllen, *Chem. Eur. J.* **2002**, *8*, 4475–4492.
[23] A. Adolf, M. Gonsior, I. Krossing, *J. Am. Chem. Soc.* **2002**, *124*, 7111–7116.
[24] I. Krossing, H. Brands, R. Feuerhake, S. Koenig, *J. Fluorine Chem.* **2001**, *112*, 83–90.
[25] I. Krossing, I. Raabe, *Angew. Chem.* **2001**, *113*, 4544–4547; *Angew. Chem. Int. Ed.* **2001**, *40*, 4406–4409.
[26] I. Krossing, *Chem. Eur. J.* **2001**, *7*, 490–502.
[27] M. Gonsior, I. Krossing, *Dalton Trans.* **2005**, 2022–2030.
[28] B. W. Tattershall, E. L. Sandham, *J. Chem. Soc. Dalton Trans.* **2001**, 1834–1840.
[29] A. Bihlmeier, M. Gonsior, I. Raabe, N. Trapp, I. Krossing, *Chem. Eur. J.* **2004**, *10*, 5041–5051.
[30] T. Bjorholm, H. J. Jakobsen, *J. Am. Chem. Soc.* **1991**, *113*, 27–32.
[31] M. Kaupp, C. Aubauer, G. Engelhardt, T. M. Klapötke, O. L. Malkina, *J. Chem. Phys.* **1999**, *110*, 3897–3902.
[32] The Al–O distances and Al–O–C angles in **2b** [1.723(2), 1.724(2), 1.728(2), 1.728(2) Å, 147.0° on average] and in **2a** [1.704(11), 1.720(10), 1.718(9), 1.739(10) Å, 150.0° on average] lie in the typical range for an $[Al(OR)_4]^-$ ion, for example in $Ag[Al(OR)_4]^-$.
[33] The contacts *s* (in valency units v.u.) are defined as $s=(R/R_0)^{-N}$, where *R* is the observed distance, R_0 is the covalent bond distance (bond order = 1) of the bond in question, and *N* is an empirically derived constant. For S···F contacts, $N=3.8$ and $R_0=1.55$ Å: I. D. Brown, in *Structure and Bonding in Crystals* (Eds.: M. O'Keefe and A. Navrotsky), Academic Press, London, **1981**, vol. 2, p. 1.
[34] Y.-Q. Yu, C. L. Stumpf, H. I. Kenttamaa, *Int. J. Mass Spectrom.* **2000**, *195/196*, 609–623.
[35] Y.-Q. Yu, *Application of Fourier transform ion cyclotron resonance mass spectrometry to reactivity studies of phosphenium ions ($ClPCl^+$ and $CH_3OP^+OCH_3$) and isomeric 2,3-and 2,5-dihydrofuran radical cations*, Ph.D. thesis, Purdue University, West Lafayette, IN, USA, **2000**, p. 169
[36] L. E. Ramirez-Arizmendi, Y. Q. Yu, H. I. Kenttamaa, *J. Am. Soc. Mass Spectrom.* **1999**, *10*, 379–385.
[37] H. L. Sievers, H.-F. Grützmacher, P. Caravatti, *Int. J. Mass Spectrom. Ion Processes* **1996**, *157/158*, 233–247.
[38] D. Gudat, *Eur. J. Inorg. Chem.* **1998**, 1087–1094.
[39] L. Latifzadeh-Masoudipour, K. Balasubramanian, *Chem. Phys. Lett.* **1997**, *267*, 545–550.
[40] L. Latifzadeh, K. Balasubramanian, *Chem. Phys. Lett.* **1996**, *258*, 393–399.
[41] L. Latifzadeh, K. Balasubramanian, *Chem. Phys. Lett.* **1994**, *228*, 463–470.
[42] N. Burford, C. A. Dyker, A. Decken, *Angew. Chem.* **2005**, *117*, 2416–2419; *Angew. Chem. Int. Ed.* **2005**, *44*, 2364–2367.
[43] N. Burford, A. D. Phillips, H. A. Spinney, M. Lumsden, U. Werner-Zwanziger, M. J. Ferguson, R. McDonald, *J. Am. Chem. Soc.* **2005**, *127*, 3921–3927.
[44] N. Burford, D. E. Herbert, P. J. Ragogna, R. McDonald, M. J. Ferguson, *J. Am. Chem. Soc.* **2004**, *126*, 17067–17073.
[45] N. Burford, P. J. Ragogna, R. McDonald, M. J. Ferguson, *J. Am. Chem. Soc.* **2003**, *125*, 14404–14410.
[46] M. Gee, R. E. Wasylishen, P. J. Ragogna, N. Burford, R. McDonald, *Can. J. Chem.* **2002**, *80*, 1488–1500.
[47] "PI_2^+" and P_2I_4 could give two products: $I_2P–PI_2^+–PI_2$ (P–P insertion or coordination) and $I_3P^+–PI–PI_2$ (P–I insertion). However, we could not distinguish between these possibilities, since the migration of "I^+" is likely to be very rapid and only one product was isolated even at −78 °C: the $I_2P–PI_2^+–PI_2$ isomer.
[48] M. Baudler, D. Grenz, U. Arndt, H. Budzikiewicz, M. Feher, *Chem. Ber.* **1988**, *121*, 1707–1709.
[49] a) Programs WINNMR and WINDAISY, Bruker Daltonic, Bremen, **1999**; b) G. Hägele, M. Engelhardt, W. Boenigk, *Simulation und automatisierte Analyse von NMR-Spektren*, VCH, Weinheim, **1987**.
[50] M. von Arnim, R. Ahlrichs, *J. Chem. Phys.* **1999**, *111*, 9183–9190.
[51] R. Ahlrichs, M. Bär, M. Häser, H. Horn, C. Kölmel, *Chem. Phys. Lett.* **1989**, *162*, 165–169.
[52] F. Weigend, M. Häser, *Theor. Chim. Acta* **1997**, *97*, 331–340.
[53] A. Schäfer, C. Huber, R. Ahlrichs, *J. Chem. Phys.* **1994**, *100*, 5829–5835.
[54] A. Schäfer, H. Horn, R. Ahlrichs, *J. Chem. Phys.* **1992**, *97*, 2571–2577.
[55] W. Kuechle, M. Dolg, H. Stoll, H. Preuss, *Mol. Phys.* **1991**, *74*, 1245.
[56] A. Klamt, G. Schürmann, *J. Chem. Soc. Perkin. Trans. 2* **1993**, 799–805.
[57] Gaussian 03, Version 6.0, M. J. Frisch, G. W. Trucks, H. B. Schlegel, G. E. Scuseria, M. A. Robb, J. R. Cheeseman, J. A. Montgomery, Jr., T. Vreven, K. N. Kudin, J. C. Burant, J. M. Millam, S. S. Iyengar, J. Tomasi, V. Barone, B. Mennucci, M. Cossi, G. Scalmani, N. Rega, G. A. Petersson, H. Nakatsuji, M. Hada, M. Ehara, K. Toyota, R. Fukuda, J. Hasegawa, M. Ishida, T. Nakajima, Y. Honda, O. Kitao, H. Nakai, M. Klene, X. Li, J. E. Knox, H. P. Hratchian, J. B. Cross, C. Adamo, J. Jaramillo, R. Gomperts, R. E. Stratmann, O. Yazyev, A. J. Austin, R. Cammi, C. Pomelli, J. W. Ochterski, P. Y. Ayala, K. Morokuma, G. A. Voth, P. Salvador, J. J. Dannenberg, V. G. Zakrzewski, S. Dapprich, A. D. Daniels, M. C. Strain, O. Farkas, D. K.

Malick, A. D. Rabuck, K. Raghavachari, J. B. Foresman, J. V. Ortiz, Q. Cui, A. G. Baboul, S. Clifford, J. Cioslowski, B. B. Stefanov, G. Liu, A. Liashenko, P. Piskorz, I. Komaromi, R. L. Martin, D. J. Fox, T. Keith, M. A. Al-Laham, C. Y. Peng, A. Nanayakkara, M. Challacombe, P. M. W. Gill, B. Johnson, W. Chen, M. W. Wong, C. Gonzalez, J. A. Pople, Gaussian, Inc., Pittsburgh, PA, **2003**.

[58] T. S. Cameron, R. J. Deeth, I. Dionne, H. Du, H. D. B. Jenkins, I. Krossing, J. Passmore, H. K. Roobottom, *Inorg. Chem.* **2000**, *39*, 5614–5631.

[59] H. D. B. Jenkins, L. C. Jitariu, I. Krossing, J. Passmore, R. Suontamo, *J. Comput. Chem.* **2000**, *21*, 218–226.

[60] I. Krossing, J. Passmore, *Inorg. Chem.* **1999**, *38*, 5203–5211.

Received: February 8, 2005
Revised: September 20, 2005
Published online: December 20, 2005

